J Mater Sci: Mater Electron (2015) 26:7109–7116
DOI 10.1007/s10854-015-3333-4

CrossMark

# Study of dielectric relaxation processes in printable zinc oxide films on transparent substrates

**Sharmistha Paul**[1,3] · **Paul G. Harris**[1] · **Ashwani K. Sharma**[2] · **Asim K. Ray**[1]

Received: 19 March 2015 / Accepted: 5 June 2015 / Published online: 17 June 2015
© Springer Science+Business Media New York 2015

**Abstract** AC impedance spectroscopic measurements have been performed on sol–gel derived zinc oxide (ZnO) films on transparent fluorine-doped tin oxide coated glass substrates in the frequency range $10^{-2}$ to $10^{6}$ Hz over the temperature range −185 to +25 °C (88–298 K). The relaxation behaviour of the nanocrystal line ZnO thin film can be described in terms of the Debye model giving an interpretation of the semi-circular relaxation phenomenon within the given temperature range. Two different relaxation times were obtained from impedance (Z) and electric modulus (M) studies of the devices and the multiple hopping of charge carriers between trap sites in grain and grain-boundary regions is believed to be responsible for charge transport. The values of activation energies for trap levels obtained from AC conductivity study are 0.0153 and 0.0487 eV which are close to the activation energies obtained from DC electrical measurement for temperature region between 88 and 178 K and 179 and 298 K, respectively.

## 1 Introduction

Zinc oxide (ZnO) is an *n* type semiconductor with a direct band gap of 3.4 eV and has been extensively studied for its applications in optoelectronics [1], spintronics [2], nano electronics [3, 4], solar cells [5, 6] and biosensors [7]. The study of charge transport mechanisms in a ZnO thin film containing defects, both for doped and undoped cases, is very important to determine the suitability of its electrical, optoelectronic properties for specific applications [8]. Variable range hopping (VRH) was found to be responsible for charge transport in polycrystalline ZnO sputtered films on a glass substrate under different oxygen pressures showed over a wide range of temperature from liquid helium temperature to 300 K. However, the exponential dependence of steady state conductivity $\sigma_{DC}$ on temperature T followed a $T^{-1/2}$ law at relatively high temperatures but a $T^{-1/4}$ dependency became prevalent at low temperatures due to the presence of a Coulomb gap in oxygen deficient films [9]. Similarly, temperature dependence of $\sigma_{DC}$ of chemical vapour deposited ZnO films was investigated in the presence of oxygen containing water vapour for the temperature range from 87 to 297 K, using the four probe method. Thermionic and thermal field emissions over grain boundaries were found to be responsible for linear Arrhenius plot type band conduction above 170 K. The variable range hopping conduction became, on the other hand, a prevalent mechanism at low temperatures below 170 K [10].

Dielectric relaxation spectroscopy which involves the examination of AC electrical response over a wide frequency range provides information on the conductivity of thin films of wide range materials in terms of structural homogeneity and stability considering relative contribution of grain, grain boundary and defect states [11]. The real and imaginary parts of complex impedance (*Z*), complex permittivity (*ε*), complex electric modulus (*M*) obtained from the AC response are usually plotted in complex plane and then modelled in an equivalent circuit comprising

✉ Asim K. Ray
Asim.Ray@brunel.ac.uk

1 Institute of Materials and Manufacturing, Brunel University London, Uxbridge, Middlesex UB8 3PH, UK

2 Res Laboratory, Space Vehicles Directorate, Se Kirtland AFB, USAF, Albuquerque, NM 87117, USA

3 West Bengal State Council of Science and Technology, Bikash Bhavan, North Block, Kolkata 700091, India

resistance ($R$), capacitance ($C$) and constant phase element (CPE) [12, 13]. Nyquist or Cole–Cole, Davidson-Cole plots, the graphical representations of frequency dependent complex dielectric parameters, are useful for analysis of one or more well separated relaxation processes in materials following Debye or non-Debye dielectric behaviours [14–16]. The mechanism of electronic conduction in ZnO film at temperatures above the room temperature has been reported in the literature as the transfer of electrons from interstitial Zn atoms and $O_2$ vacancies which are acting as donor levels to the conduction band [17]. Dielectric spectroscopy was employed in the temperature range between 113 and 473 K to study the defect relaxation process in ZnO ceramics. The appearance of relaxation processes at temperature below 243 K are believed to be associated with intrinsic interstitial zinc and oxygen vacancies which are not susceptible to additives and impulse current degradation. The electric properties of the ZnO ceramics are related to high temperature relaxation processes above 353 K which are influenced by additives and grain boundaries [18].

Using commercially available zinc oxide (ZnO) nanoparticles, the low cost fabrication of ZnO memristors with a high off–on ratio of $2.2 \times 10^4$ has recently reported by us [19]. When spin-coated ZnO films on transparent glass slides were annealed at 500 °C in air for 2 h, the formation of Wurtzite hexagonal polycrystalline structure was observed from Raman and X-Ray diffraction Spectra. The grain sizes were found to increase from ~36 to ~112 nm on annealing possibly due to amorphous hydrated species on the particle surface being converted back to zincite. In the present paper, the electrical properties of Au/ZnO/FTO devices have been studied using AC impedance spectroscopy in order to determine physically interesting parameters such AC and DC conductivities, relaxation time, electric modulus in the temperature varying from 88 to 298 K over the frequency ranges between $10^{-2}$ and $10^6$ Hz. The activation energies have been determined for different donor levels of ZnO films for different temperature and frequency ranges and these values have then been compared with the results obtained from DC current–voltage measurements.

## 2 Experimental

For the formulation of thin films, fluorine-doped tin oxide (FTO) coated glass slides (TEK 15, Pilkington UK) with surface resistivities of ~15Ω/square were used as substrates. A small volume of a 40 wt% dispersion of ZnO nanoparticles (<130 nm) in ethanol (Sigma-Aldrich) was spun at 250 and 2000 rpm in sequence for 15 and 60 s respectively, to deposit thin films on ultrasonically cleaned FTO substrates. The solvent was then completely removed by oven drying the films at 120 °C for 15 min. The fabrication and materials characterisation of the devices has been described earlier [19]. Subsequently the samples were ramped (over a 30 min period) up to 500 °C in air and held at this temperature for 2 h before being ramped down to room temperature. The samples were examined using a Zeiss Supra 35VP field emission scanning electron microscope (FESEM). A 10 keV beam was used in conjunction with an in-lens secondary electron detector system. A gold (Au) layer was sputtered via a mask to form the top electrode for the Au/ZnO/FTO sandwich structure. A Keithley 617 electrometer and an Oxford instruments constant temperature liquid nitrogen cryostat were used in a microprocessor controlled measuring system to record DC current–voltage curves from ZnO films sandwiched between FTO coated glass slides and evaporated gold electrodes, in vacuum of $10^{-4}$ mbar over the temperature range of 88–298 K. The voltage was applied to the sample through the Au electrode from −2 to 2 V with scan rate 500 mV/s keeping the FTO electrode grounded. The complex impedance of the Au/ZnO/FTO device was measured using an impedance analyser (Solartron 1260, UK) in the frequency range of $10^{-2}$ to $10^{-6}$ Hz, signal amplitude 0.1 V rms and over the temperature range 88–298 K.

## 3 Results and discussion

### 3.1 DC measurements

The DC current versus voltage characteristics of a Au/ZnO/FTO device under varying temperature conditions from 88 to 298 K are shown in Fig. 1. The voltage was scanned from −2 to +2 and then back to −2 V with scan rate 500 mv/s. As shown in the inset in Fig. 1, the variation of current density $J$ (A/m$^2$) with electrical field $E$ (V/m) on logarithmic scales is linear for different temperatures, taking data from a half cycle of 0–2 V and it is clear that the two terminal device exhibits Ohmic conduction. Figure 2 shows the Arrhenius plots of DC conductivity, $\sigma_{DC}$ as a function of inverse temperature T in Kelvin over the temperature range from 88 to 298 K. Two temperature regimes exist corresponding to the cross-over temperature 208 K, each with a different value of activation energy E according to the Arrhenius exponential equation in the form:

$$\sigma_{DC} = \sigma_0 \exp(-E/kT) \quad (1)$$

where $k$ is the Boltzmann constant and $\sigma_0$ is the pre exponential factor, representing the conductivity at infinite temperature. Similar two regimes of temperature dependent DC conductivity have been reported for ZnO thin films

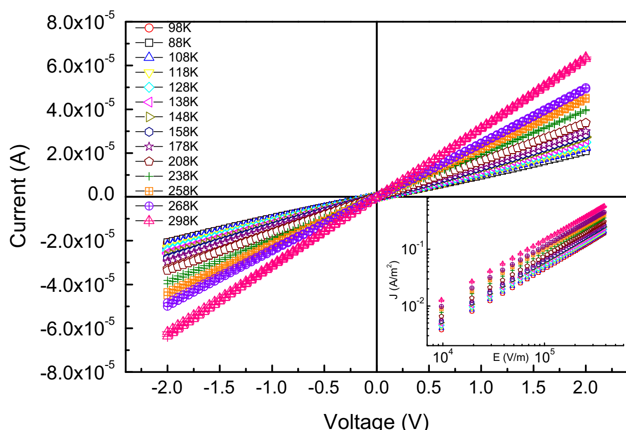


**Fig. 1** Current–Voltage plot of Au/ZnO/FTO device over the temperature range 88–298 K for one complete cycle from −2 to 2 V for scan rate 500 mV/s. *Inset* shows current density versus electric field for the same from 0 to 2 V in log scale

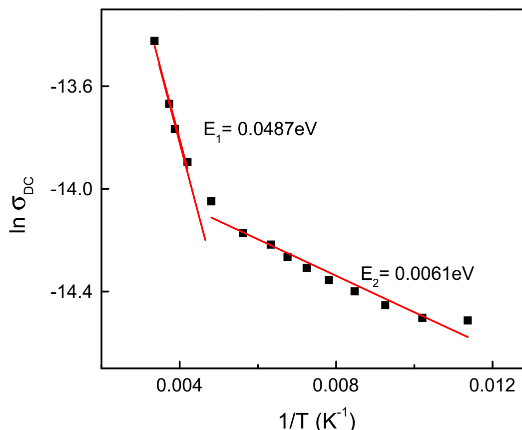


**Fig. 2** DC conductivity plot with inverse of temperature for Au/ZnO/FTO device at 2 V. *Squares* are experimental points while *lines* are resulted after linear fit

grown by the pulsed laser deposition technique [20]. Values of E are estimated to be 6.1 meV ($E_2$) and 48.7 meV ($E_1$) from the slopes of linear fits to experimental data for the two temperature region of 88–208 and 208–298 K, respectively. The high temperature activation energy value is consistent with one obtained for hydrothermally grown ZnO film [21]. The thermally activated DC conductivity, $\sigma_{DC}$, follows a linear Arrhenius behaviour, indicating conduction of electrons in extended states beyond the mobility edge for the temperature range of 208–298 K, as shown in Fig. 2. For the temperature range 88–208 K, the conductivity deviates from the thermally activated Arrhenius plot, which suggests that variable range hopping conduction between localized states is occurring. Variable range hopping conduction of localized electrons following Mott equation in the ZnO film has been reported before in literature, in the temperature range of 87–295 K [22].

### 3.2 AC measurements

#### 3.2.1 Impedance formalism

Impedance spectroscopy is a simple analytical tool to determine electrical conductivity through various parameters like complex impedance ($Z^*$), complex electric modulus ($M^*$), complex dielectric permittivity ($\varepsilon^*$). These parameters are correlated [12] as given by:

$$M^*(\omega) = j\omega C_0 Z^*(\omega) = M'(\omega) + jM''(\omega) \quad (2)$$

$$\varepsilon^*(\omega) = M^*(\omega)^{-1} \quad (3)$$

where $\omega$ is the angular frequency, and $C_0$ the vacuum capacitance of the measuring thin film of ZnO, i.e., $C_0 = \varepsilon_0 (A/d)$, $\varepsilon_0$ is the permittivity of free space, $A$ and $d$ are the

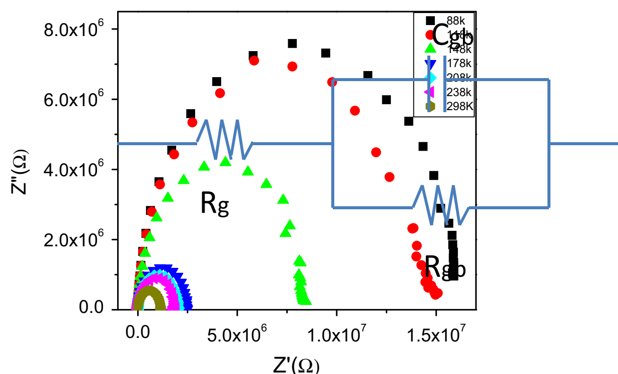


**Fig. 3** Nyquist plot ($Z'$ vs $Z''$) at various temperatures of Au/ZnO/FTO device and proposed R–C circuit model (*inset*)

area and thickness of the film, respectively. For detailed investigation of electrical properties, impedance measurements were carried out in the frequency range of 0.01–1 MHz and for the temperature range of 88–298 K. Figure 3 shows the complex plane plot of the real part of impedance ($Z'$) versus imaginary part of the impedance ($Z''$) for a Au/ZnO/FTO device at 0 V DC. The resistive and capacitive properties of the grain boundary region of ZnO films can easily be calculated using the equivalent circuit model and a non-linear least square curve fitting approach, to the observed single and slightly depressed semi-circular plot [12]. The arcs and semicircles having their centres lying below and on the $Z'$ axis, with the rise of temperature in Fig. 3, intersect the right hand side of $Z'$ axis at resistance values corresponding to grain boundary region $R_{gb}[Z' = R_{gb} = R_{DC}\, as\, \omega \rightarrow 0]$. The equivalent circuit of the system can be proposed by considering grain resistance $R_g$ in series with the parallel RC component of grain boundary region. The value of $R_g$ is obtained directly from

the high frequency intercept of the impedance arc on the $Z'$ axis. Further, a reduction in the size of the semi-circular arc with a rise in temperature was observed, consistent with decreasing values of $R_g$ and $R_{gb}$ similar to those reported by Sahay et al. [23].

From this impedance plot, a relaxation time constant ($\tau_z$) has been calculated from the summits of each curves following $\omega_m \tau_z = 1$, where $\omega_m$ is the summit frequency. The capacitance of the grain boundary region, $C_{gb}$, can be calculated from $\tau_z$ using the relation $\tau_z = R_{gb} C_{gb}$. The variation of $\tau_z$ with reciprocal of temperature is shown in Fig. 4 and has been fitted according to the Arrhenius equation:

$$\tau_z = \tau_{0z} \exp(-E/kT) \quad (4)$$

where $E$ is the activation energy associated with relaxation process, $\tau_{0z}$ is the characteristic relaxation time factor, k is the Boltzmann constant and T is the temperature. The achieved values of activation energies for trap levels for two temperature regions after linear fit are found to be $E_1 = 0.0553$ eV (179–298 K) and $E_2 = 0.0105$ eV (88–178 K) which are close to values obtained from DC conductivity in Fig. 2. Calculated $\tau_{0z}$ value ($\tau_{0z1} = 7.485 \times 10^{-6}$, $\tau_{0z2} = 3.02769 \times 10^{-4}$) suggests a multiple hopping charge carrier conduction mechanism in the grain and grain boundary region. In general, the relaxation time constant is larger in the grain boundary region ($\tau_{0z2}$) than the grain region ($\tau_{0z1}$) [24]. The average grain size of ZnO is found to be 75 nm from the SEM image of the ZnO film (upper inset of Fig. 4). It is thought that a high conduction path is created due to the presence of a large defect density in the interfacial region although grain boundaries may act as hindrance to charge transport. Dissipation or loss factor $D$, deduced from the relation $D = Z'/Z''$, is plotted against temperature in the lower inset of Fig. 4. $D$ was found to be influenced by both frequency and temperature, reaching a minimum at $10^5$ Hz. The dissipation factor increases with temperature up to ~200 K. However, this effect becomes less pronounced with further temperature rises.

The variation of grain boundary resistance $R_{gb}$ and capacitance $C_{gb}$ with temperature are depicted in Fig. 5. From the slopes of Arrhenius plot of $R_{gb}$ two energy levels are obtained, the first one located below the conduction band at 0.047 eV (temperature region 179–298 K) and the second one at 0.011 eV (temperature region 88–178 K). Similarly, from the slopes of Arrhenius plot of $C_{gb}$ in the same figure, the activation energy for two donor levels are found, the first was 0.102 eV and the second 0.021 eV.

The variation of $Z', Z''$ as a function of frequency at different temperatures is plotted in Fig. 6a, b. It is observed from Fig. 6a that $Z'$ decreases with the increase in frequency as well as temperature. The $Z'$ values for all temperatures merge above $10^4$ Hz. The variation of the imaginary part of impedance ($Z''$) with frequency at different temperatures is shown in Fig. 6b. This indicates that $Z''$ reaches a maximum which shifts towards the higher frequency region with an increase in temperature, indicative of losses in the ZnO thin film. The peak position of $Z''_{max}$ in Hz is plotted against temperature in the inset of Fig. 6b.

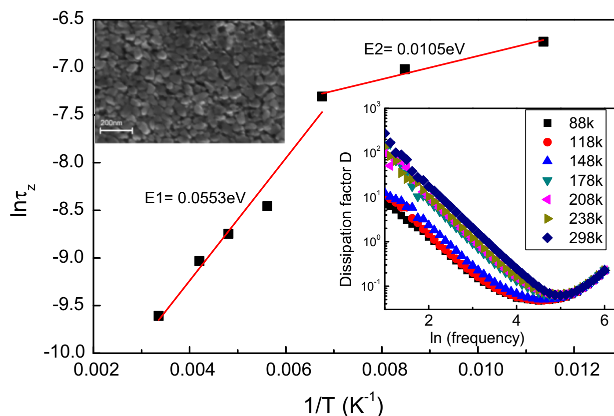


**Fig. 4** Variation of relaxation time ($\tau_z$) with reciprocal of temperature of Au/ZnO/FTO device. *Upper inset* shows SEM image of ZnO film. *Lower inset* shows variation of dissipation factor (D) with temperature

### 3.2.2 Electric modulus plots

Defect relaxation of the Au/ZnO/FTO structure can be analysed with the help of a complex electric modulus ($M$) plot. The real $M'$ and imaginary $M''$ parts of the complex electric modulus were calculated from the measured impedance data following Eqs. 2 and 3. Figure 7a, b shows the variation of $M', M''$ with frequency at different temperatures. As observed from Fig. 7a, the value of $M'$ is near zero in the low frequency region, started dispersed in the mid frequency region and reached maximum in the high frequency region for all temperatures. This behaviour can be explained by short range mobility of charge carriers [25]. Figure 7b reveals the plot of $M''$ with frequency at different temperatures. A single peak is observed whose position shifts towards high frequency with an increase in temperature (inset Fig. 7b). This may be explained by thermally activated dielectric relaxation, where hopping process of charge carriers are dominating in the film due to the combination of grain and grain boundary effects [26, 27]. The long range mobility of charge carriers could be determined by consideration of the frequency of the maxima. It is likely that they are confined to potential wells, and are only mobile over short ranges at frequencies after the peak maxima.

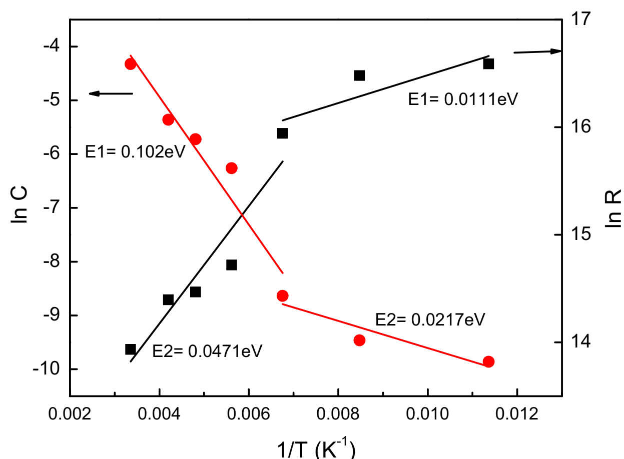


**Fig. 5** Variation of grain boundary resistance $R_{gb}$ and capacitance $C_{gb}$ with temperature

The peak position of $Z''_{\max}, M''_{\max}$ with frequency over the temperature range 88–298 K are located at same position as depicted in the insets of Figs. 6b and 7b. It can be predicted that the peak position of normalized parameters $Z'/Z''_{\max}, M'/M''_{\max}$ are located at same frequency. The type of dielectric response can be predicted from the degree of overlapping peak position of $Z'$ and $M'$ curves [28]. According to Debye theory, for an ideal dielectric relaxation case, impedance and electric modulus maxima peak position are predicted to be at the same frequency. Long range relaxation and information about delocalized states can be predicted from the overlapping peak position of $Z'/Z''_{\max}$ and $M'/M''_{\max}$. It is evident from asymmetric nature of $M'/M''_{\max}$ curve that the conduction mechanism in this film may be regulated by lattice defect and structural irregularities.

Figure 8 displays the relationship between $M'$ and $M''$ at different temperatures. The presence of single and slightly depressed semicircles confirms the presence of multiple relaxation times [29]. Relaxation time constants ($\tau_M$) have been calculated from the maxima of each of the curves following $\omega_m \tau_M = 1$ and fitted to an Arrhenius equation. The activation energy values for two defect levels were found from two different temperature regions to be $E_1 = 0.0487$ eV (179–298 K) and $E_2 = 0.0153$ eV (88–178 K) which are consistent with values obtained from DC conductivity in Fig. 2 and within error limit of 10 % as obtained from $Z'$ to $Z''$ plot in Fig. 3. The relaxation time constants ($\tau_{0M}$) obtained for these levels are $\tau_{0M1} = 1.026 \times 10^{-5}$, $\tau_{0M2} = 1.674 \times 10^{-4}$. These results support the view that multiple hopping of charge carriers among defects (Zn, $O_2$ vacancies) in the ZnO film is occurring.

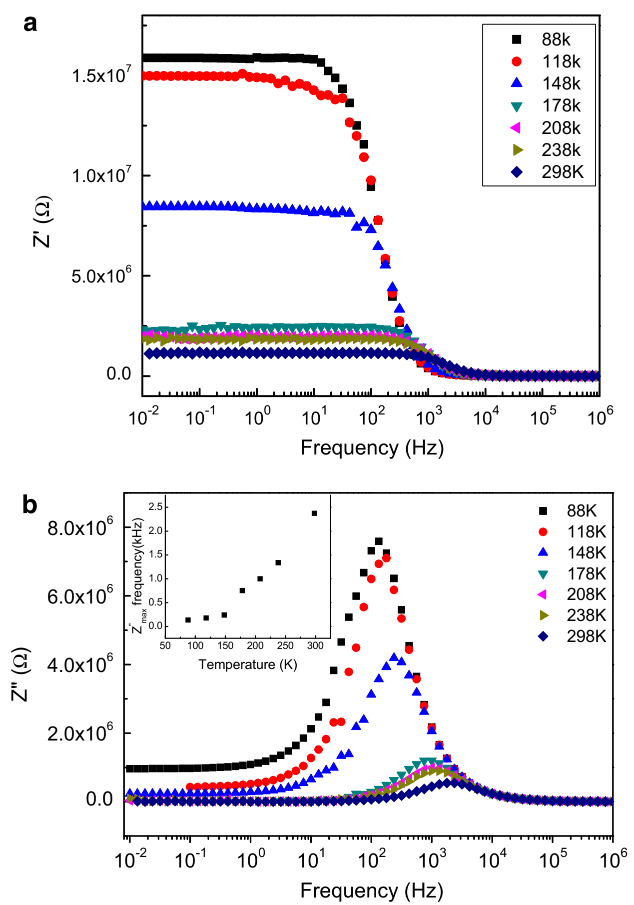


**Fig. 6** Variation of **a** $Z'$, and **b** $Z''$ with frequency at different temperature. *Inset* of **b** shows variation of $Z''_{\max}$ frequency with temperature

### 3.2.3 AC conductivity

AC conductivity $\sigma_{AC}$ due to localized states in a dielectric material can be written as [30].

$$\sigma_{AC}(\omega) = \sigma_{DC} + A\omega^s \tag{5}$$

where $\omega$ is the angular frequency, $\sigma_{DC}$ is the DC conductivity when $\omega \to 0$, $A$ is pre factor, and $s$ is frequency exponent lying between $0 < s < 1$. Both $A$ and $s$ are weakly dependent on temperature. Figure 9 shows a logarithmic plot of the AC conductivity of the Au/ZnO/FTO device as a function of $\omega$ for various temperatures from 88 to 298 K. From this figure it is evident that the conductivity of the device is frequency and temperature dependent. There are four frequency regions according to the linear relationship between AC conductivity and frequency which are separated by lines as shown in Fig. 9. These are region I (1 MHz–600 kHz), region II (600–10 kHz), region III (10–3 kHz) and region IV (3 kHz–$10^{-2}$ Hz). At high frequency, conductivity has almost the same value irrespective of temperature. However, the effect of measuring

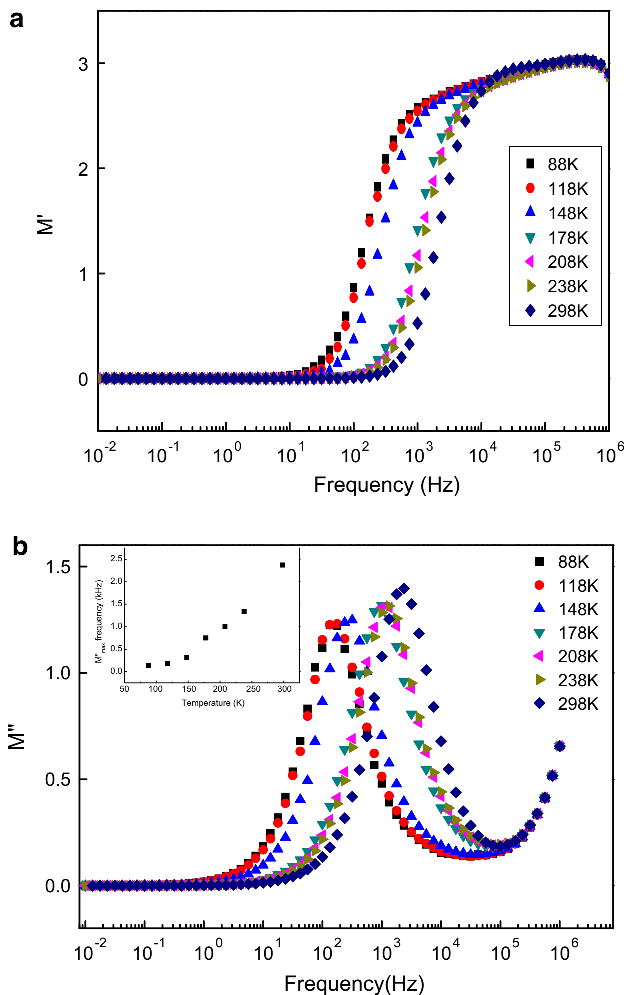


**Fig. 7** Variation of **a** $M'$, and **b** $M''$ with frequency at different temperatures. *Inset* of **b** shows variation of $M''_{\max}$ frequency with temperature

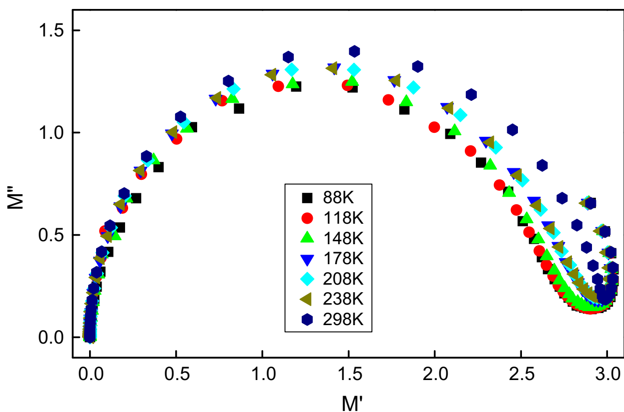


**Fig. 8** Variation of $M'$ with $M''$ at different temperatures

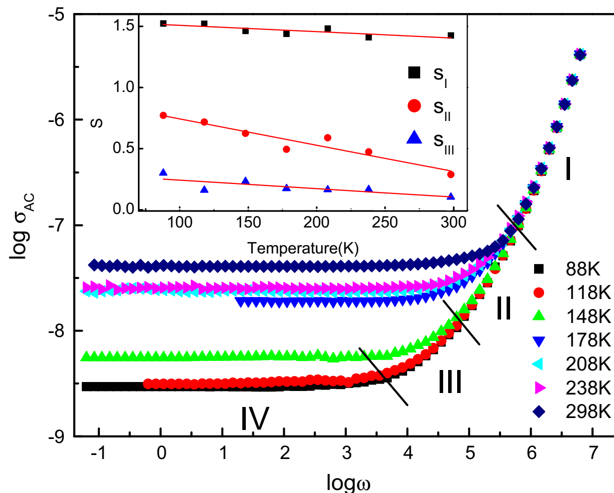


**Fig. 9** Variation of AC conductivity ($\sigma_{AC}$) of Au/ZnO/FTO device as a function of angular frequency (ω) for various temperatures from 88 to 298 K. *Inset* shows variation of *s* with temperature in different frequency regions

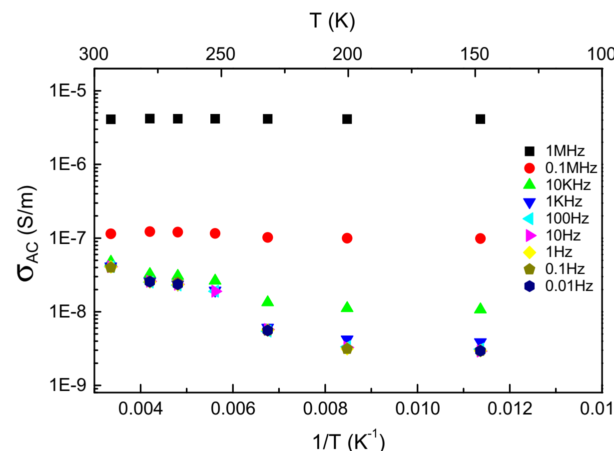


**Fig. 10** Variation of AC conductivity with reciprocal of temperature for Au/ZnO/FTO device in the frequency range of 0.01 Hz–1 MHz

temperature is prominent at lower frequencies. The change in behaviour of the AC conductivity, from initially flat to rapidly rising may be attributed to a change in the hopping behaviour of the charge carriers, from long range to short range [31]. When a single charge particle moves across multiple barriers, the resultant conductivity will show multiple steep rises as a function of frequency [13]. The value of *s* obtained after linear fit of Eq. 5 in frequency region I, II, III is plotted against temperature in the inset of Fig. 9. It is evident from the graph that hopping movement involves translational motion of charge carriers ($s < 1$) and

**Table 1** Activation energy calculation for trap levels from various parameters

| Parameter | Plot method | Energy for trap level (eV) | |
|---|---|---|---|
| | | $E_1$ (from temperature region I 179–298 K) | $E_2$ (from temperature region II 88–178 K) |
| Relaxation time constant $\tau_z$ | Arrhenius plot of $\tau_z$ | 0.0553 | 0.0105 |
| | | $\tau_{0z1} = 7.485 \times 10^{-6}$ | $\tau_{0z2} = 3.02769 \times 10^{-4}$ |
| Grain boundary resistance $R_{gb}$ | Arrhenius plot of $R_{gb}$ | 0.047 | 0.011 |
| Grain boundary capacitance $C_{gb}$ | Arrhenius plot of $C_{gb}$ | 0.102 | 0.021 |
| Relaxation time constants $\tau_M$ | Arrhenius plot of $\tau_M$ | 0.0487 | 0.0153 |
| | | $\tau_{0M1} = 1.026 \times 10^{-5}$ | $\tau_{0M2} = 1.674 \times 10^{-4}$ |
| AC conductivity $\sigma_{AC}$ for frequency range (0.01 Hz–1 kHz) | Arrhenius plot of $\sigma_{AC}$ | 0.0453 ± 0.002 eV | 0.0108 ± 0.001 eV |
| DC conductivity $\sigma_{DC}$ | Calculated $\sigma_{DC}$ from $\sigma_{AC}$ (when $\omega \rightarrow 0$) | 0.0471 | 0.0111 |
| DC conductivity $\sigma_{DC}$ | DC measurement (0–2 V) | 0.0487 (208–298 K) | 0.0061 (88–208 K) |

localized hopping for carriers without leaving the neighbourhood ($s > 1$) [32]. Therefore conductivity involves both long range and short range or localized types of hopping process. When values of $\sigma_{DC}$ (when $\omega \rightarrow 0$) are calculated from Fig. 9 and then fitted against Eq. 1, values of 0.0471 (for 179–298 K) and 0.0111 eV (for 88–178 K) are estimated for activation energy. These values agree satisfactorily with those obtained from DC measurements in Fig. 2. The variation of AC conductivity with the inverse of temperature in the frequency range of 0.01 Hz–1 MHz is depicted in Fig. 10. It is evident from this graph that conductivity increases with temperature for all frequencies. This may be due to hopping of thermally activated charge carriers between localized states of different energy levels. The variation of AC conductivity with temperature is independent of frequency below 1 kHz. This behaviour may be due to the intrinsic nature of the conductivity of the material. The activation energies for trap levels calculated from this figure for the frequency range (0.01 Hz–1 kHz) from two temperature regions are 0.0453 ± 0.002 (for 179–298 K) and 0.0108 ± 0.001 eV (for 88–178 K) which are similar to the values obtained from DC measurement.

## 4 Conclusions

Commercially available ZnO nanoparticles were employed to produce an active thin ZnO layer sandwiched between an FTO substrate and a top electrode of sputtered Au film, forming a two terminal Au/ZnO/FTO device. The electrical behaviour of this device has been studied with the help of AC impedance and DC measurements in the frequency range $10^{-2}$ to $10^{6}$ Hz and a temperature range −185 to 25 °C (88–298 K). Using the Arrhenius plots, the activation energies have been calculated for relaxation time constant, grain boundary resistances and capacitances. Table 1 summarises the values of activation energies for two different trap levels from different parameters and it can be seen that values of activation energies for the AC parameters are in agreement with those values obtained from the DC parameters. This suggests that conduction is due to multiple hopping processes between a number of different trap sites within the grain/grain boundary regions.

**Acknowledgments** This work is sponsored by the Air Force Office of Scientific Research, Air Force Material Command, USAF, under Grant No. FA8655-08-1-3056.

## References

1. A.B. Djurisic, A.M.C. Ng, X.Y. Chen, Prog. Quantum Electron **34**(4), 191 (2010)
2. M. Opel, S.T.B. Goennenwein, M. Althammer, K.W. Nielsen, E.M. Karrer-Muller, S. Bauer, K. Senn, C. Schwark, C. Weier, G. Guntherodt, B. Beschoten, R. Gross, Phys. Status Solidi B-Basic Solid State Phys. **251**(9), 1700 (2014)
3. J.H. Song, Y. Zhang, C. Xu, W.Z. Wu, Z.L. Wang, Nano Lett. **11**(7), 2829 (2011)
4. Q. Yang, Y.P. Wu, Y. Liu, C.F. Pan, Z.L. Wang, Phys. Chem. Chem. Phys. **16**(7), 2790 (2014)
5. S.Q. Bi, F.L. Meng, Y.Z. Zheng, X. Han, X. Tao, J.F. Chen, J. Power Sources **272**, 485 (2014)
6. J. Huang, Z.G. Yin, Q.D. Zheng, Energy Environ. Sci. **4**(10), 3861 (2011)
7. R. Ahmad, N. Tripathy, N.K. Jang, G. Khang, Y.B. Hahn, Sens. Actuator B-Chem. **206**, 146 (2015)
8. C.-H. Yang, Y. Kuo, C.-H. Lin, Appl. Phys. Lett. **96**(19), 192106 (2010)
9. Y.L. Huang, S.P. Chiu, Z.X. Zhu, Z.Q. Li, J.J. Lin, J. Appl. Phys. **107**, 063715 (2010)
10. Y. Natsume, H. Sakata, T. Hirayama, Phys. Status Solidi (a) **148**, 485 (1995)
11. A. K. Jonscher, J. Phys. D: Appl. Phys. **32**(14), R57 (1999)
12. J.R. Macdonald, *Impedance Spectroscopy-Emphasizing Solid Materials and Systems* (Wiley, New York, 1987)
13. M. Li, A. Fetiera, D.C. Sinclair, J. Appl. Phys. **98**, 084101 (2005)

14. L.L. Hench, J.K. West, *Principles of Electronic Ceramics* (Wiley, Singapore, 1990)
15. K.S. Cole, R.H. Cole, J. Chem. Phys. **19**, 1484 (1951)
16. S. Havnhk, S. Negami, Polymer **8**, 161 (1967)
17. E. Ziegler, A. Heirich, H. Opperman, G. Stover, Phys. Status Solidi (a) **66**, 635 (1981)
18. X. Zhao, J. Li, H. Li, S. Li, J. Appl. Phys. **111**, 124106 (2012)
19. S. Paul, P.G. Harris, C. Pal, A.K. Sharma, A.K. Ray, Mater. Lett. **130**, 40 (2014)
20. S.P. Heluani, G. Braunstein, M. Villafuerte, G. Simonelli, S. Duhalde, Thin Solid Films **515**(4), 2379 (2006)
21. C.C. Lien, C.Y. Wu, Z.Q. Li, J.J. Lin, J. Appl. Phys. **110**(6), 063706 (2011)
22. Y. Natsume, H. Sakata, T. Hirayama, H. Yanagida, J. Appl. Phys. **72**(9), 4203 (1992)
23. P.P. Sahay, S. Tewari, R.K. Nath, S. Jha, M. Shamsuddin, J. Mater. Sci. **43**, 4534 (2008)
24. D.C. Sinclair, T.B. Adams, F.D. Morrison, A.R. West, Appl. Phys. Lett. **80**, 2153 (2002)
25. B.K. Singh, B. Kumar, Cryst. Res. Technol. **45**, 1003 (2010)
26. K. Prabakar, S.K. Narayandass, D. Mangalaraj, Mater. Sci. Eng. B-Solid State Mater. Adv. Technol. **98**(3), 225 (2003)
27. E. Iguchi, K. Idea, W.H. Jung, Phys. Rev. B **54**, 17431 (1996)
28. R. Tripathi, A. Kumar, C. Bharati, T.P. Sinha, Curr. Appl. Phys. **10**(2), 676 (2010)
29. R. Gerhardt, J. Phys. Chem. Solids **55**, 1491 (1994)
30. A.K. Jonscher, *Universal Relaxation Law* (Chelsea Dielectric Press, London, 1996)
31. R.H. Chen, R.Y. Chang, C.S. Shem, Solid State Ion. **177**, 2857 (2006)
32. K. Funke, Prog. Solid State Chem. **22**, 111 (1993)